Lecture Notes for:
Accelerator Physics and Technologies for Linear Colliders

Physics 575, Chapter 9 "Ground Motion"
University of Chicago
March 5, 2002

Vladimir Shiltsev
Fermi National Accelerator Laboratory
(Batavia, IL)

Contents:

1. Introduction in Ground Motion
   a) GM in time and space, fractals
   b) waves and creeps, T° and P effects
   c) PSD and RMS, correlation and coherence

2. Vibration Sensors:
   a) human hand
   b) geophone
   c) Linear Collider

3. Vibration control:
   a) site and tunnel
   b) support structures
   c) damping pads
   d) active stabilization of elements
   e) beam-based feedback

Problems for Chapter 7, Physics 575

9.1 Introduction in Ground Motion

Beam trajectory stability is of great relevance to e^+ e^+ linear colliders (LC). Motion of the magnets and accelerating structures may cause significant luminosity degradation due to beam offset at the interaction point. Additionally, LCs may suffer from the beam emittance (beam size) growth induced by vibration of the elements. For these reasons, it is necessary to understand the effect of the ground motion induced element jitter on the beam motion. While this occurs mainly at frequencies above 1 Hz, slow element position drifts necessitate regular element re-alignment. To estimate required frequency of this procedure, spatial and temporal properties of ground motion need to be understood.

9.1.a. Ground Motion in Time and Space

Ground motion is known to be very time and site dependent, so the best way to reveal its general properties (and hide true details) is to look at the Log(A)-Log(1/T) plot in Fig.1 where the logarithm of amplitude of the motion in meters is plotted versus logarithm of inverse time in seconds for different processes.

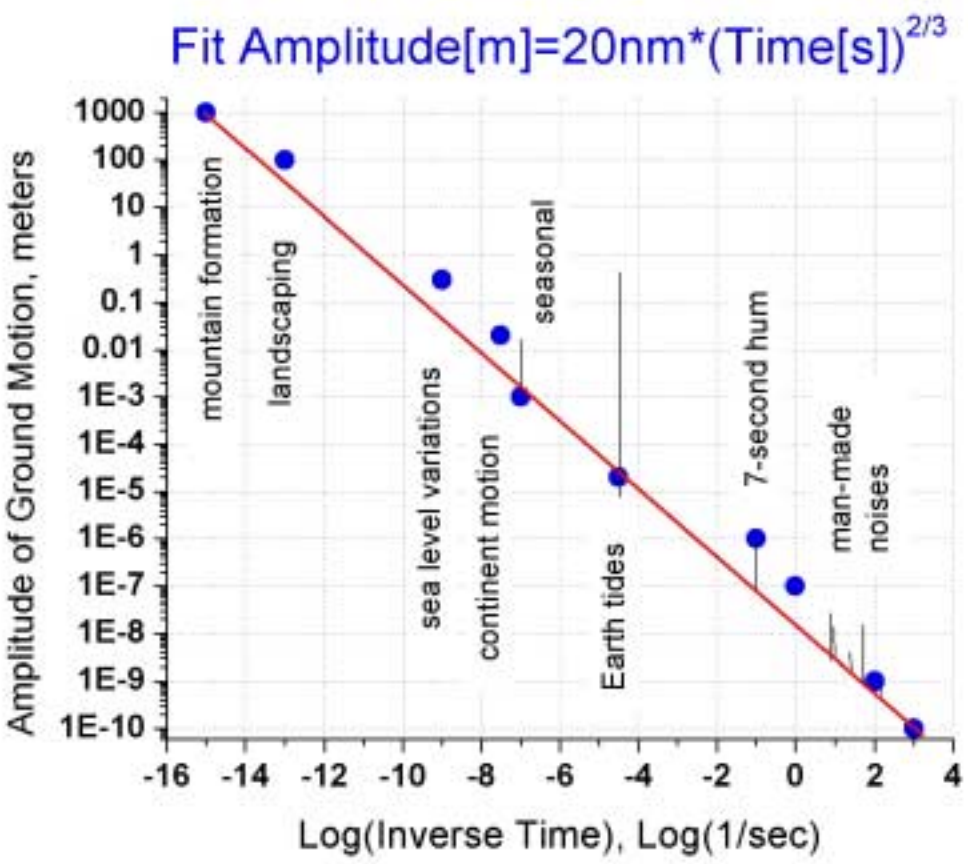

Figure 1: Log-Log plot of ground motion.

For example, the top left point in the beginning of the plot corresponds to the formation of mountains, 1000 meters high, over some 30 million years or 1e+15 seconds. At the other end of the plot, we have 1 Angstrom (1e-4 micrometer, 1e-10 meter) ground vibration at a frequency of 1kHz=1000Hz, or a period of 0.001 sec. The most remarkable feature of the plot is that the amplitude of the motion decreases with a decrease of the time interval. Simple-minded fit of the data is A=20[nm]*T^{α} [sec], where the power α is close to 2/3. The latter is very important for understanding where the energy which shakes the ground comes from. Indeed, if we consider the motion of the ground as an ensemble of processes at different time scales T_n, then the energy of each process is:

$$E_n = m_n v_n^2/2 \propto T_n^{2\alpha-2} \qquad (9.1),$$

where we assume the total mass of the ground m_n is the same for all types of motion, and we estimate the ground velocity as $v_n = 2\pi A_n/T_n$. The total energy is the sum of energies in all n processes

$$E_{total} = \Sigma E_n \propto T_{max}^{2\alpha-1} \qquad (9.2).$$

Therefore, for any α larger than ½, the longest time period motion has most of the ground motion energy. One can say that the ground motion takes energy out of long term processes - those caused by steady Solar heat flux of about 1300 W/m^2 and heat flux of about 0.1W/m^2 from inner parts of the Earth – and then the energy goes into shorter and shorter time processes until final dissipation. It is interesting to note that if α would be less than ½, then $E_{total} \propto T_{min}^{\ 2\alpha-1}$ and most of the energy would be contained in short term processes. A marginal case of α=½ corresponds to uniform distribution of energy among all time scales.

Power law distributions are common for fractals, and the ground motion is a multi-fractal in time and space with all the characteristic statistical properties of such processes.

9.1.b Waves and Creeps, Temperature and Pressure Effects

In a number of cases the motion of the ground is quite regular and, therefore, predictable. For example, there are few remarkable peaks in Fig.1: the first one at 3e-7 sec corresponds to motion due to annual temperature variation. For the Chicago area, the average seasonal ΔT is about 20 ^{o}C, thermal skin depth D of the ground affected by annual variations is about 5-10 meters, that results in motion of about $\Delta Y = \gamma D \Delta T \approx 1\text{-}2$ mm for a typical thermal expansion coefficient of $\gamma \approx 10^{-5}$ 1/ ^{o}C. The next peak in Fig.1 is for Earth tides which happen twice a day due to gradient in gravitational attraction forces of the Moon and Sun. Tides have a wavelength of ½ of the Earth circumference $\lambda_{tide} \approx 20000$ km and typical amplitude of vertical land surface displacement is $A_{tide} \approx 0.3$m (latitude dependent). Relative displacement for two points L meter apart - also called the <u>first difference</u> $\Delta Y(L) = (Y(z) - Y(z+L))$ - is small $\Delta Y = 2A_{tide} \sin(\pi L / \lambda_{tide}) \approx A_{tide} 2\pi L / \lambda_{tide}$, (also dependent on the direction of the vector L) that gives some 20 microns over L=180 meters (600 ft) which unnoticeable for humans but can be easily detected by geophysical instruments (tilt-meters) – as shown in Fig.2 a). The horizontal axis is time in days in December 2000 (e.g., 31.96 corresponds to late night of December 31, 2000), while the vertical axis is for a relative vertical position of two observation points 180 meters apart in a 300 ft deep dolomite tunnel (total scale is 895-813=82 micrometers). Because of periodic changes in relative positions in the system Moon-Earth-Sun, the amplitude of diurnal oscillations varies with a period of 14 days – it is obviously less at the beginning of the plot and in the middle of the month. Obvious creep (slow change of the tilt) of the order of 82 microns/180 meters=0.5 microrad is seen over 1 month in the same plot. Possible explanations for this change are: natural geological instability, temperature effect or atmospheric pressure effect.

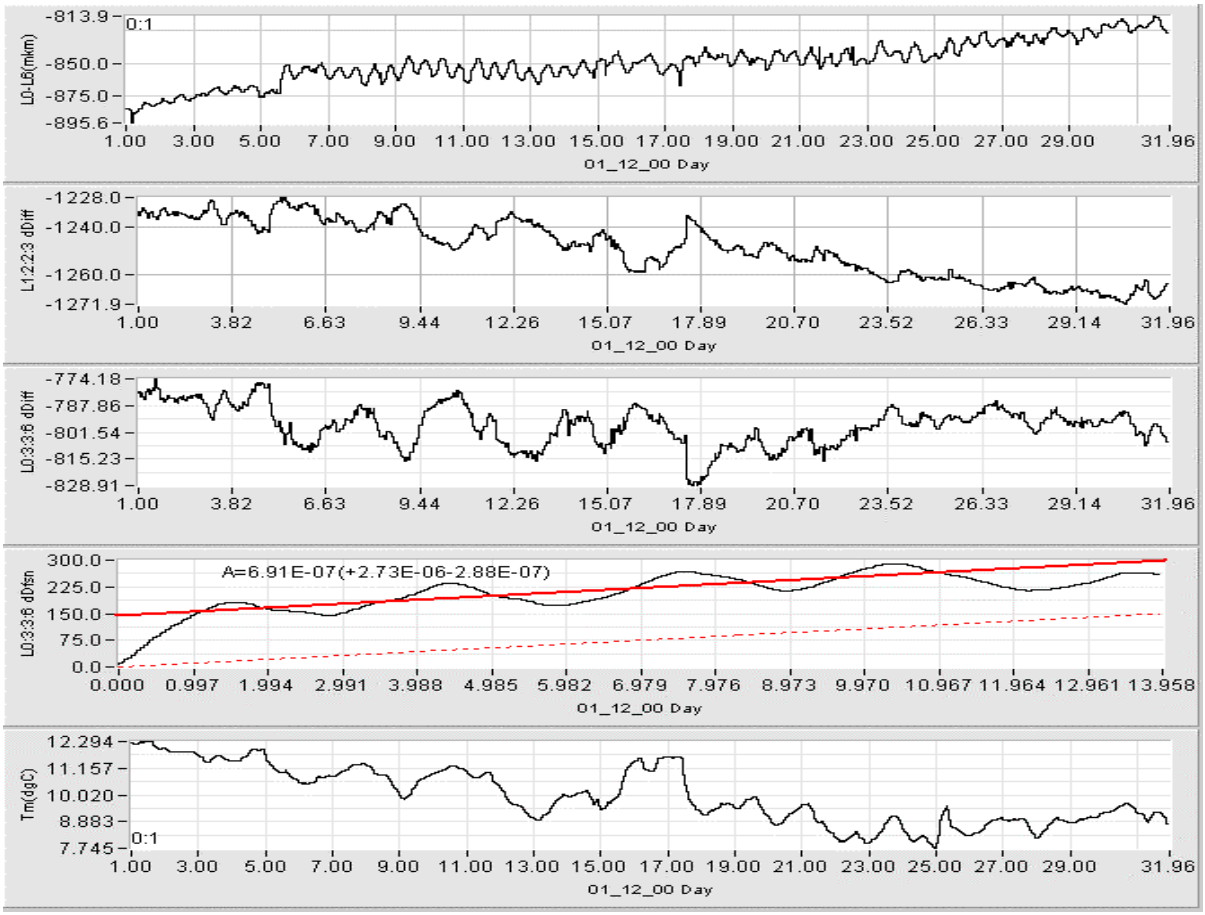

Figure 2: Slow ground motion in 300 ft deep dolomite mine (Aurora, IL) in December , 2000. Top to bottom a) to e), comments in the text.

Even in underground facilities like accelerator tunnels or in deep mines with fresh air circulation there are significant daily and weekly variations of air; for example, Fig.2 e) reveals 1^{o}C variations in the Aurora mine daily and some 4^{o}C drop in the temperature over 3 weeks (from 12.3^{o}C to 7.7^{o}C).

To separate the temperature effects from the tides, one can use *the second difference* $\Delta^2 Y\,(L)=(\,\Delta Y(z)-\,\Delta Y(z+L))=\,Y(z)-2\,Y(z+L)+Y(z+2L)$. Indeed, for the tides, the second difference over hundreds of meters is very small $\Delta^2 Y \approx A_{\,tide}\,(2\pi L/\,\lambda_{\rm tide})^{\,2} \approx$ 1 nm (assuming the media is elastic). Fig.2 b) and c) show that, respectively, $\Delta^2 Y\,(30\ m)$ and $\Delta^2 Y\,(90m)$ are both correlated with average temperature changes with coefficients about –20 micron/ ^{o}C and +40 micron/ ^{o}C correspondingly. Air pressure also can contribute into the motion of the ground, both in these $\Delta Y\,(L)$ and $\Delta^2 Y\,(L)$ but usually over longer distances $L \geq 1$ km. From definitions, it is obvious that the first difference reflects mostly tilt variations while the second difference is a better measure of fractures in the ground.

Besides regular Earth tides and temperature drifts, the ground does move randomly for no obvious reasons. Such a diffusion is a natural

settlement process which takes place at all spatial and temporal scales. It is a manifestation of energy release in the ground (described above): energy is pushed into the ground at longer time/space scales while it dissipates at very small scales. *ATL law* (which is more of a handy formulae rather than an established physical law) estimates the mean squared relative diffusive ground displacement as

$$<\Delta X^2>=A\times T\times L \quad (9.3)$$

where A is a site/ground/depth dependent coefficient of the order of 10^{-7} … 10^{-5} $\mu m^2/s/m$, T is time interval between measurements, L is distance between observation points and brackets <…> mean average over time and space. Contrary to tides and thermal expansion, the diffusive motion is about the same in horizontal and vertical planes. There are indications that the ATL law is valid over periods from an hour to a few years and over distances from meters to several kilometers. For such a process, the mean square of the second difference is twice the mean square of the first difference $<(\Delta^2 X)^2>=2<\Delta X^2>$. Fig.2 d) shows the mean square of the second vertical difference for points 90 meters apart, and the red line presents linear fit $<(\Delta^2 X(L=90))^2> = 150 + 2\ A\times T\times L$, with $A= 6.9\times 10^{-7}\mu m^2/s/m$ and T up to 14 days. Somewhat excessive motion at short periods $T<1$ day can be explained by ground jumps due to almost daily blasts taking place in that mine (within 1 mile from the measurement system location) – many of them with amplitudes of 10 to 25 microns are seen in the Fig.2 a).

Other less predictable and more powerful blasts happen all the time in many places in the world – those are earthquakes. Illinois is not a seismically active place but large amplitude seismic waves (20 to several hundred microns) with periods between 20 to 60 seconds are coming here almost every month from other parts of the US and the world. These events last for tens of minutes because different types of waves from the same earthquake come with different delays. Fortunately (or – unfortunately?) due to the long wavelength of dozens of kilometers, these waves do not excite significant relative motion of the ground ΔX at distances L less than a kilometer – the same effects as for the tides – and thus, are unnoticeable to humans and, as we will see later, for accelerators.

Let us finish with regularities in the ground motion. Fig. 1 shows a peak named "7 second" hum. That remarkable phenomena is often wrongfully associated with ocean waves hitting beaches while, in fact, it is excited by storms in open oceans. Motion of huge masses of water create ground waves which penetrate even into the central parts of continents. Typical amplitude of these waves in Chicago varies from 0.1

to 1 micron; but, again, due to the dozens kilometer wavelength, the "7-second hum" (actually, containing all frequencies from 0.1 to 1 Hz) is unnoticeable.

Finally, man made vibrations are represented in Fig.1 by the number of peaks between 1 and a few hundred Hz. The amplitude of these vibrations depends on the power of the source and the distance from it.

9.1.c Power Spectral Density and Root Mean Square, Correlation and Coherence

By definition, power spectral density (PSD) of ground motion $z(t)$ (z stands for either x or y) is equal to

$$P(\omega)=\lim (1/T)\left|\int z(t)\, exp(-it\omega)dt\right|^2 \qquad (9.4).$$

Since measured data consist of real numbers only then $P(\omega)=P(-\omega)$. PSD in real frequency $f=\omega/2\pi$ (always positive) is often more convenient $P(f)=4\pi P(\omega=2\pi f)$ and refers to the root mean squared (RMS) value of the ground motion in frequency band from f_0 to f_1 as

$$\sigma(f_0, f_1)=\sigma(f_0 < f < f_1) = \left[\int P(f)df\right]^{1/2} \qquad (9.5).$$

The dimension of the PSD is length^2/frequency= micrometer^2/Hz. Fig. 3 presents the PSD for higher frequency ground motion measured at several accelerators worldwide.

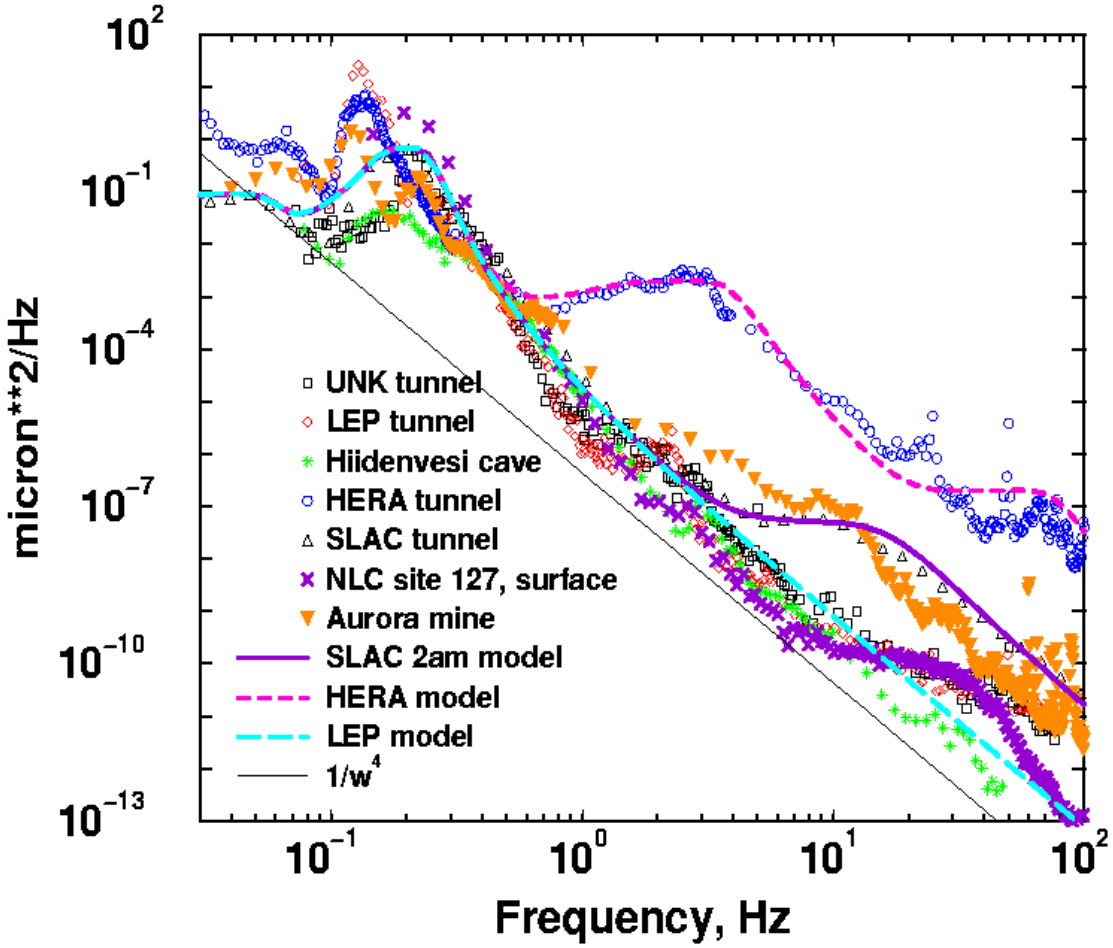

Figure 3: Power Spectral Density of ground motion measured at different accelerator sites.

The large spread in the data (two orders in the PSD at microseismic peak around 0.2 Hz, and four orders above 30 Hz) is a characteristic feature of high frequency ground motion – it is dependent on many factors and not very predictable. There is no single scaling law for the presented spectra as they scale somewhere between $1/f^4$ and $1/f^2$. Since $\sigma(f \to 0) \to \infty$, ground motion is a *non-stationary* noise process.

Fig.4 shows values of $\sigma(f, \infty)$ – integrated amplitude – for some places. One can see that the amplitude of the ground motion above 1 Hz does not exceed 0.1 micron=100 nm.

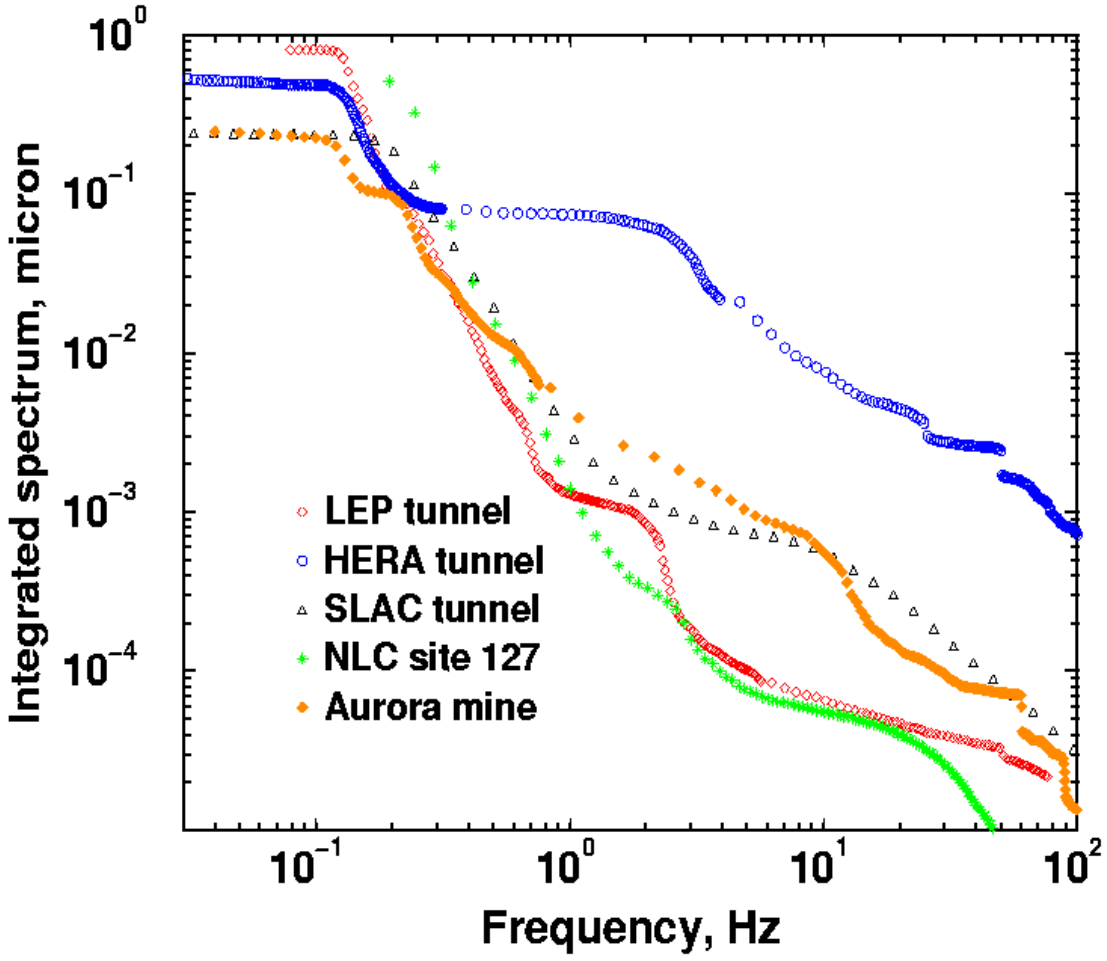

Figure 4: RMS ground vibration amplitude $\sigma(f, \infty)$ vs frequency f.

The mutual power spectrum of two signals $z_1(t)$ and $z_2(t)$ (e.g., signals measured simultaneously at two different locations) is defined as

$$P_{12}(\omega)=\lim (1/T) \int\int z_1(t)\, z_2((t')\, exp(-i\omega(t-t'))\, dtdt' \qquad (9.6).$$

The spectrum of correlation $C_{12}(\omega)$ (complex quantity) and spectrum of coherence $H_{12}(\omega)$ of two signals $z_1(t)$ and $z_2(t)$ are equal to

$$C_{12}(\omega)=<P_{12}(\omega)>/[<P_{11}(\omega)><]P_{22}(\omega)>]^{1/2} \ , \ H_{12}(\omega)=|C_{12}(\omega)| \qquad (9.7),$$

where brackets <…> stand for average over many measurements (for a single measurement $H_{12}(\omega)=1$).

Usually, for natural ground motion the correlation tends to be 1 at lower frequencies and smaller distances. High frequency ground vibrations at frequencies above 1 Hz are usually not well correlated over distances exceeding the wavelength $\lambda_f \approx v(f)/f$ unless a strong unique source of vibrations is around. A simple model of multiple random, uncorrelated

sources uniformly distributed over a 2D surface gives the correlation between two points of ground L meter apart

$$\text{Re } C_{12}(f)=J_0\,[2\pi L\, f / v(f)\ ]\ ,\ \text{Im } C_{12}(f)=0 \qquad (9.10),$$

that satisfactorily describes reality (J_0 is Bessel function). Ground wave velocity v depends on site geology, depth and frequency. At very low frequencies and significant depth, it can be as large as 2-4 km/s, while on the surface it can be less than 500 m/s . Consequently, a significant drop of correlation occurs at ten(s) of meters on the surface and at hundred(s) meters in hard rock tunnels.

9.2 Vibration sensors

Vibration measuring instruments can respond to displacement x, velocity $v=x\omega$ or acceleration $a=x\omega^2$.

9.2.a Human hand (for free)

Glabrous skin (hands) has an epidermal layer of about 1.5 mm in thickness and a dermis of about 3 mm. Meissner corpuscles are located in the dermis of glabrous skin – see Fig.5. They respond to pressure variations caused by vibrations and are most sensitive in 20-40 Hz range. As pressure is just force divided by area $P=F/S$, and force is mass multiplied by acceleration $F=ma$, then the human hand is *an accelerometer*.

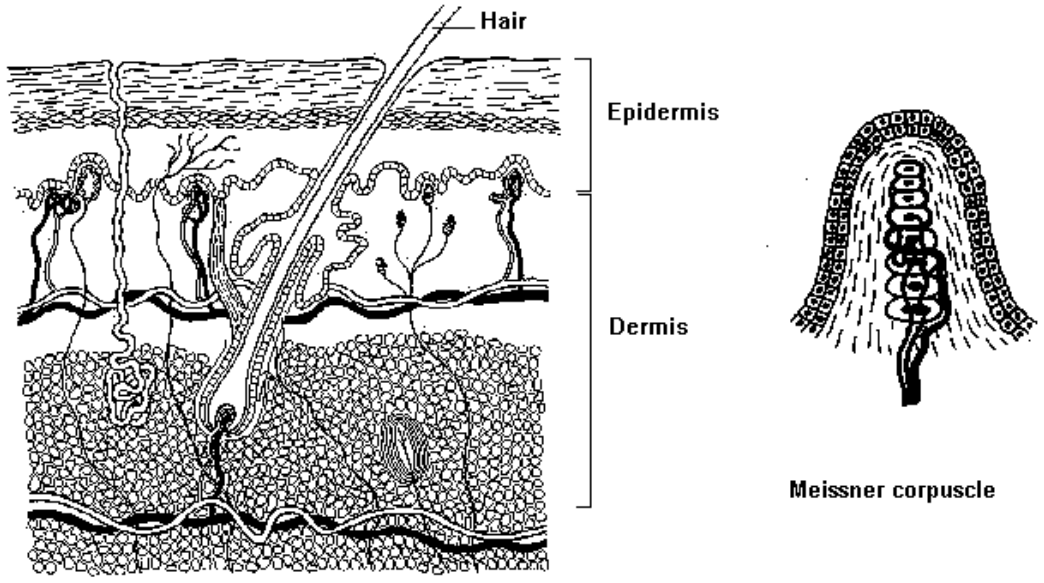

Figure 5: Human skin and Messiner corpuscle

And not a bad one . The “rule of thumb” is that if you feel vibrations by hand then the amplitude of vibrations is 1 micrometer or more. From there

one may calculate a detection threshold of the hand to be $a = \omega^2 x$=0.004 m/s^2 that is 0.4% of g. Typical industrial accelerators are not much better in noise amplitude but they cover a much larger frequency band from a few dozen Hz to a few kHz. The better accelerometers used for geophysics research are about 100 times more sensitive. Ambient natural ground motion acceleration at f=30 Hz is some 1/1,000,000 of g.

What makes biological systems, such as our hands, so sensitive even compared with electronic devices? Recently it was proposed that it's because of the active way of the measurement called *stochastic resonance* which allows detection of tiny signals by introducing controlled noise into the system. Experiments with mechanoreceptors of the crayfish, *Procambarus clarki*, indicate the validity of the model and similar experiments with the human sensory system are underway.

9.2.b Geophone (few k$)

Geophone is *velocity-meter* to measure vertical or horizontal vibrations. An example is shown in Fig.6. It consists of a pendulum (1) attached to the base of the probe (2) by supporting springs (3). Motion of the base forces the pendulum and a coil attached to it to move in the field of a permanent magnet (4). So, the voltage induced in the coil is proportional to the coil velocity.

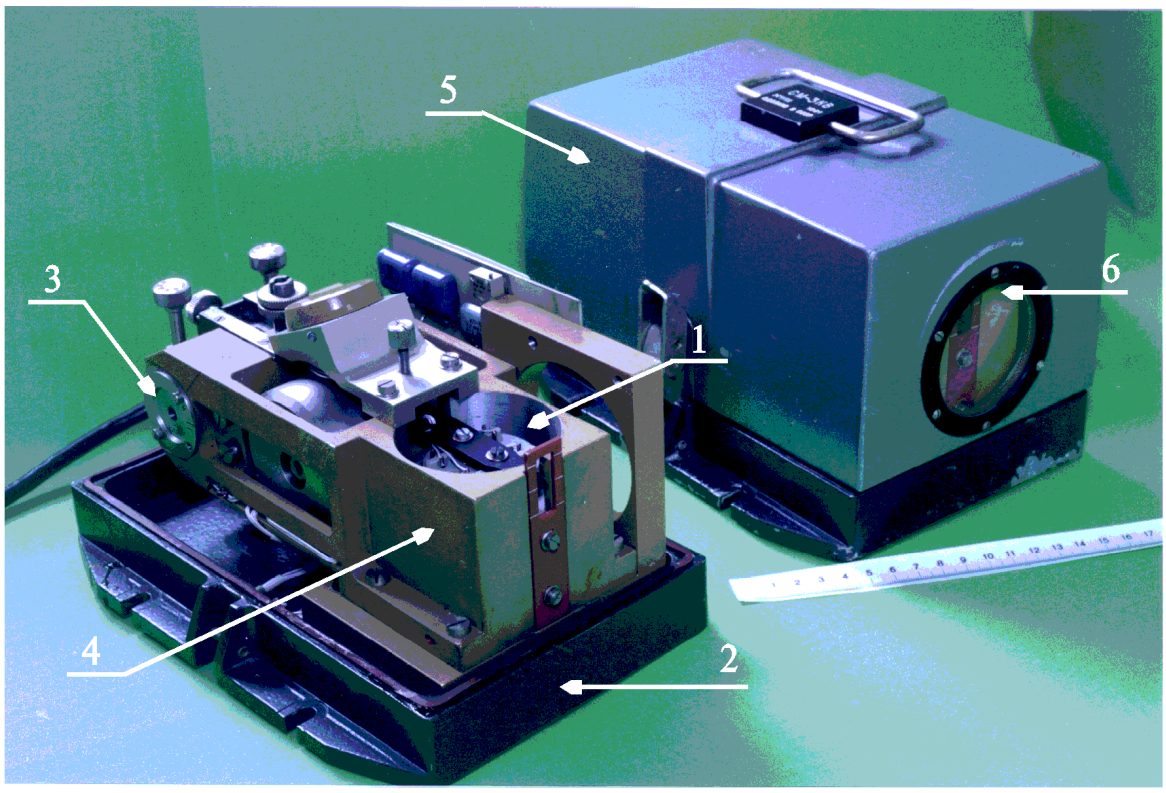

Figure 6: Seismometer of SM3 - KV type. 1- pendulum with signal and feedback coils, 2 - base of the probe, 3 - springs attaching pendulum to the base, 4 - permanent magnet, 5 - probe box, 6 -window to watch the pendulum.

The pendulum resonance frequency is f=2 Hz and a quality factor Q=12. Without modifications it is used to work as a *velocity-meter* at frequencies from 2 to 40 Hz. To extend the frequency band as low as 0.05 Hz and up to 100 Hz this seismometer was modified by introducing an electronic negative feedback system – see Fig.7. This system allows it to eliminate the influence of the intrinsic pendulum resonance at 0.5 Hz, and also to improve the linearity, dynamical range and sensitivity of the probe. The gain of the feedback loop is intentionally reduced below 0.05 Hz to cut low frequency noises and above 100 Hz to avoid excitation of parasitic mechanical resonances. An equivalent probe input rms noise of 0.02 micron/s is -10db to -100dB of the natural ground motion over the whole frequency range of the probe.

The principle of the negative feedback is going to be widely used in future Linear Collider(s) for the stabilization of important elements (magnets) and beam trajectory stabilization.

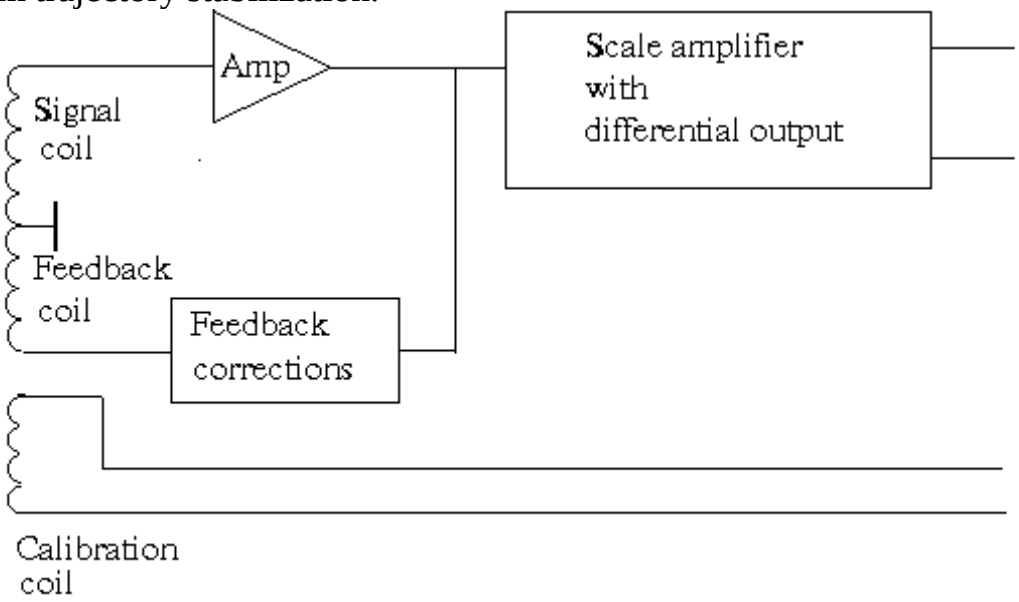

Figure 7: Block diagram of seismometer negative feedback system.

9.2.c Linear Collider (few billion $)

The Linear Collider consists mainly of large numbers of regular FADA cells (F- focusing quadrupole magnet, A- accelerating structure, D – defocusing quadrupole). Transverse *displacement* of any element creates a betatron

wave downstream of the linac $z(s)$ which is proportional to the original angular kick θ_i

$$z_i(s) = \theta_i [\beta(s)\,\beta(s_i)]^{1/2}\ \sin(\varphi(s)-\varphi(s_i)),\ s > s_i \qquad (9.11),$$

where $\beta(s)$ is the beta-function and $\varphi(s)=\int ds/\beta(s)$ is the betatron phase. For example, if a focusing quadrupole with focal length F_i is displaced by dz_i from its original "ideal" position, then $\theta_i = dz_i / F_i$. The typical value of F_i is 10-30 meters. Accelerating structures also produce defocusing kicks for off-centered beams, which are proportional to the beam current and dependent on the geometry of the structure (which is different for different Linear Collider projects). These kicks are usually much less than for the same displacement of quadrupoles, by a factor of 10 to a few hundreds, depending on the LC design parameters. But, they are dangerous because the kick is different in different parts of the bunch (smaller at the head and stronger in the center and in the tail).

If we consider the very end of the accelerator $s=s_e$, then the beam displacement is a superposition of all tiny kicks along the way – from the injection to the end $z(s)=\Sigma z_i(s)$. If the angular kicks θ_i are always in phase with the beam betatron motion (e.g. due to ground waves with wavelength $\lambda_f \approx 2\pi<\beta(s)>$) then beam position jitter at the end will be proportional to the total number of quadrupoles in the linac N_q : $|z(s)| \approx N_q <[\beta(s)\,\beta(s_i)]^{1/2}> |\theta_i|$. For example, a 1 micron beam displacement – about the rms vertical beam size at the end of the NLC - can be caused by as small as a 5 Angsrom=0.5 nm ground wave ($N_q \approx 600$, $<[\beta(s)\,\beta(s_i)]^{1/2}> \approx 30$ m $<F_i> \approx 10$ m) propagating along the linac. To have proper wavelength of some 150 m, the wave frequency should be around 7-14 Hz. Fortunately, as we mentioned above, natural ground motion at such frequencies is uncorrelated even over 10-20 meters, so the ground wave model is usually not appropriate for the LCs.

For completely uncorrelated motion of quadrupoles with the rms value of σ one gets

$$<z(s_e)^2> \approx 2\, N_q\, \beta(s)\, \sigma^2 / L \qquad (9.12),$$

where $L \approx 10$ m is the distance between neighbor quadrupoles. Now, $\sigma \approx 15$ nm results in the same 1 micron beam displacement at $\beta(s) \approx 50$ m. Even if we consider ground vibrations at all frequencies above 1 Hz as uncorrelated, the measured natural vibrations are still several times smaller – see Fig.4. Nevertheless, problems are expected because: a) equipment operation vibrations in the LC tunnel are expected to be (much) larger then natural levels; b) motion of the final quadrupoles near the interaction point contributes to beam-beam displacement as 1:1, so for a 3 nm vertical beam

size operation, one needs those magnets to be stabilized better than 1 nm – that is very challenging; c) longer term ground motion may have uncorrelated components exceeding amplitudes of the fast ground motion, e.g., the ATL law predicts 15 nm rms random uncorrelated displacements for neighbor quads only after $T \approx \sigma^2/A/L \approx 45$ sec for the diffusion parameter $A = 5 \times 10^{-7} \mu m^2/s/m$. After that time, the beam trajectory has to be "smoothed" by correctors or by moving the quadrupoles back to "good" positions.

9.3 Vibration control

As the ground motion (actually, vibration of elements) is of concern for the Linear Colliders, let us consider basic measures which can reduce the severity of the problem.

9.3.a Site and Tunnel

As seen from Fig.3, the ground motion is strongly site dependent and, therefore, this factor has to be taken into account while making the choice of the site. A good uniform geology layer with a harder rock would be ideal for the LC. For the same geology, a deeper tunnel is better because air pressure and temperature effects diminish with the depth. In addition, it is known that tunnels dug by tunnel boring machines are more stable than those made by blasting. Finally, as the technological equipment is a source of vibrations, one should consider all measures to keep it as far as possible from the beam line.

9.3.a Support structures

Magnets and accelerating structures must be installed on something sturdy. Usually, it is a specially designed girder platform. To avoid amplification due to mechanical resonances, it seems to be beneficial to have these girders as close to the ground as possible (An example of a good support is the Tevatron collider in Batavia, IL where the magnets lay almost on the floor (beam line is just 10" from the floor) that secures magnet well and leaves no room for resonances. Another recommendation is to use heavy girders, because some vibrations, e.g., due to cooling water flow, take place right there, on the girder. Heavier girders and, consequently, all linac elements on it, will oscillate with smaller amplitudes.

9.3.b Passive Dampers

Vibrations can be damped passively only at frequencies above 10 Hz where some materials have a significant loss factor η=(Energy Loss Per Cycle)/(Total Stored Energy). Materials with high η from 0.01 to 10 are generally not very hard and stable – examples are wood, cork, plywood, sand, rubber, plastic. Steel and Aluminum are hard materials but their loss factors are small η~0.0001 (they ring when one kicks them) and can not be used for the passive damping. Better materials are copper and hard concrete η~0.001. Recently, damping pads consisting of layers of steel intermitted with viscoelastic damping materials (VEMs, like Anatrol) have shown very good damping properties η~1 while they are quite capable of keeping pressure of a 60 tons/m^2 (100 psi). Such pads are widely used at the APS (ANL, Argonne, IL) to reduce vibration of heavy girders 3 to 10 times at frequencies of 5-15 Hz. That might be an inexpensive solution for Linear Colliders, too, though it does not solve all the problems as vibrations at other frequencies are equally important.

9.3.c Active Dampers

Active damping employs a fast analogous feedback system very similar to one used in the geophone considered above, see Fig.7. A geophone or an accelerometer should be attached to the object to stabilize (magnet or girder) and its signal is used to control the corresponding (micro)mover. In extraordinary cases, "an optical anchor" (laser position measurement system) can be used. Stabilization to a nm is possible though hard because of noises in the feedback loop. Typically such systems cover frequencies from few Hz to several dozens Hz (beyond that either noises or mechanical resonances do not allow a high gain in the loop). Active dampers are moderately expensive (on the order of 10k$ per element to stabilize) and can be used in LCs.

9.3.d Beam-based Feedback

Beam-based feedback systems have a great potential for LCs as they can eliminate detriemental effects of vibrations on the beam completely. The scheme is standard; one measures the beam displacement (locally or in several BPMs) and corrects it by fast steering dipole correctors (again, either locally or at several locations). The major drawback is their intrinsically limited natural frequency bandwidth. Indeed, the NLC will operate at the repetition rate of $f_0=1/T$=120 Hz then the Nyquist frequency for beam-based feedback will be $f_0/2$=60 Hz. Naturally, no correction of accelerator distortions will be possible for frequencies above this. The ability of the

feedback system to suppress drifts in the accelerator is a strong function of the frequency spectrum of the distortions and also depends on the design of the feedback algorithm.

Let's consider the simplest correction which assumes that any disturbance $x(t)$ is exactly corrected before the next shot of the linac. Then , the remaining distortion is just $d(t)=x(t+T)-x(t)$. Therefore, for sinusiodal distortion $x(t) = a \sin(wt)$ we have $d(t)=2 a \sin(wT/2)\cos(w(t+T/2))$. At frequencies much smaller than shot rate $f<<f_{0,}$ such systems will suppress the distortions as $|d/a| \propto 2\pi f / f_0$, but distortions will be amplified at frequencies above 1/6 of f_0 as $|d/a|>1$ and the situation may become unstable at all – depending on the spectrum of distortions at high frequencies. More sophisticated algorithms are suggested for the NLC which still allow first order suppression without significant excitation at high frequencies but the cost of that is such that algorithm suppresses only below f_0 /20 = 6 Hz. That system has been tested and routinely used at the SLC.

Linear Collider TESLA has a unique possibility: the time between bunches (a microsecond) is long enough for position measurement and successive correction; so, after only a few bunches have passed, the beams at the IP can be re-centered using similar algorithms. Thus, the bandwidth of the system f_0 /20 becomes some 50 kHz.